Enhanced Power System Damping Estimation via Optimal Probing Signal Design

S. Boersma[1], X. Bombois[2,3], L. Vanfretti [4], V. Perić[5], J-C. Gonzalez-Torres[1], R. Segur[1], A. Benchaib[1]

[1)]SuperGrid Institute SAS, 23 Rue de Cyprian, 69611 Villeurbanne, France
[2)]Laboratoire Ampère, Ecole Centrale de Lyon, 36 avenue Guy de Collongue, Ecully, France
[3)]Centre National de la Recherche Scientifique (CNRS), France
[4)] Rensselaer Polytechnic Institute, 110 8th Street, Troy, United-States
[5)]Technical University of Munich, Lichtenbergstrasse 4a, 85748 Garching

Email: sjoerd.boersma@supergrid-institute.com

Keywords

≪System Identification≫, ≪Optimal Experiment Design≫, ≪Power Systems≫, ≪Damping Estimation≫

Abstract

For real-time power system dynamic monitoring, it is important to provide accurate estimations of the network's critical electro-mechanical modes, which are time-varying frequency and damping values. This paper employs a framework for designing a multisine probing signal that, when applied in the control inputs of one of the power electronics-based grid actuators, is able to provide a damping estimation with user specified variance. The employed framework is demonstrated through simulations in a nonlinear simulator using models of varying complexity.

Introduction

Accurate monitoring of electromechanical oscillations in real-time is one of the most important functions of a wide area monitoring system [1]. Oscillations are monitored by continuously estimating the frequencies and damping ratios of dominant low-frequency electromechanical modes. These are referred to as critical system modes and, in normal operation, are damped enough such that no instability occurs. However, damping ratios of modes change over time due to time-varying operating conditions. It can occur that these damping ratios become too low for the system to remain stable under large oscillations that may arise if a severe disturbance occurs [2]. Hence it important to continuously provide an accurate mode frequency and damping estimation so that, when this crosses a specific lower bound, a controller can be activated to increase this damping, thereby preventing major system instabilities [3]. Both estimation and control are key for a smarter grid.

Approaches described in literature that provide mode estimation can roughly be divided into two categories. The first category only uses ambient excitation while, in the second category, the network is excited with a probing signal (generated by for example using a controllable power electronics device). Ambient excitation primarily comes from random load changes. This type of excitation is always present in a network and should therefore be accounted for in the damping estimation method. In general, ambient excitation is relatively low, which can easily result in estimations with relatively high variances.

The approach employed in this work is placed in the second category, *i.e.*, the network is excited with a probing signal. Results that belong to this category can be found in [4, 5, 6, 7]. In [4], injected

noise is produced by random load switching and a frequency domain identification technique is used to estimate the network's behavior. In [5], several kinds of standardized probing signals are injected in the network and corresponding damping estimations are compared. The estimations are done via Subspace Identification techniques. In [6], the authors illustrate that when applying a probing signal with frequency content close to a critical network mode frequency, the oscillations can become dangerously large. This indicates that the frequency content of the probing signal should be selected carefully. Literature on probing signal design can be found in [8, 9, 10, 11, 12]. In [8, 9, 10], the probing signal is prefiltered such that it contains specific frequency content before being injected it in the network. In [11], a multisine probing signal is considered and the phases of the multisine are optimized to obtain a probing signal with the smallest amplitude while having a user-defined power spectrum. The power spectrum of the probing signal is indeed the quantity determining the damping estimate's accuracy. Therefore, in [12], the authors design the power spectrum of a multisine probing signal (*i.e.*, the amplitudes of the different sinusoids) in such a way that an user defined accuracy of the damping estimation is ensured. This accuracy is based on the variance of the estimated damping. It is to be noted that the method in [11] can subsequently be used to also optimize the phases of the optimal multisine.

This work builds further on the work presented in [12]. The main contributions of this work are 1) the method is tested and simulated using a nonlinear power network model, 2) the optimized probing signal is actually applied to the nonlinear simulator and 3) in one test network, a high voltage direct current (HVDC) link is used to probe the network. The method employed in this work is based on the idea of running experiments for system identification while minimizing its costs. This paradigm, which has been used before in the control community [13], can be used in power system mode estimation [12]. A power spectrum of the probing signal is determined by solving an optimization problem with constraints. The objective function is defined as a weighted sum of the probing signal's power and a level of disturbance caused by probing the network. A desired level of the damping estimation's accuracy is set as a constraint. The time-domain realization of the obtained power spectrum is described by a multisine, which would be the actual probing signal applied to the network.

The remainder of this paper is organized as follows. Firstly, the utilized system identification method will briefly be described. From the estimated dynamical model, mode frequency and damping values can be evaluated. The employed method demands for probing signal selection, which is the succeeding topic in this paper. Next, the paper follows by presenting the simulation results and is then concluded.

System Identification

The prediction error method [14] is used herein as the system identification technique. Here, the network's response $y(t)$ (for example the angle difference between two buses) is assumed to be made up of the superposition of two responses (ambient and forced). The ambient system response $(\hat{H}(z)e(t))$ (with discrete time t) can be described by a monic transfer function $\hat{H}(z)$ excited by white noise $e(t)$, where the white noise represents random load changes. As stated earlier, this ambient response is always present in power networks since there are always random load changes. The forced response $(\hat{G}(z)u(t))$ is a result of exciting the network with the probing signal $u(t)$ (for example the voltage error in a SVC). Note that $\hat{H}(z), \hat{G}(z)$ will be assumed linear for the design of the probing signal. However, as mentioned in the introduction, the designed probing signal will be applied to a non-linear simulator to validate the approach.

Since both $\hat{H}(z), \hat{G}(z)$ can be derived from the same state-space model of a power system, it is reasonable to assume that both transfer functions have the same denominators. This defines the ARMAX model structure of the system:

$$y(t) = \underbrace{\frac{b(z,\theta_b)\cdot z^{-n_k}}{a(z,\theta_a)}}_{\hat{G}(z)} u(t) + \underbrace{\frac{c(z,\theta_c)}{a(z,\theta_a)}}_{\hat{H}(z)} e(t), \tag{1}$$

with $a(z,\theta_a), b(z,\theta_b), c(z,\theta_c)$ polynomials in $z \in \mathbb{C}$, $\theta_\bullet$ the parameter vectors that are found by the iden-

tification method and n_k a delay. The poles of the ARMAX model can be found by solving $a(z,\theta_a)=0$ for z and it is assumed that all poles are inside the unit circle. Let these poles be:

$$\aleph = \{z_1, z_2, \ldots, z_{n_r}, z_{n_r+1}, \bar{z}_{n_r+1}, \ldots, z_{n_r+n_i}, \bar{z}_{n_r+n_i}\}, \tag{2}$$

with $\bar{\bullet}$ the complex conjugate, n_r the number of real valued poles and n_i the number of complex pole pairs. Then define p as a subset of $\aleph$:

$$p = \{|z_1|, |z_2|, \ldots, |z_{n_r}|, z_{n_r+1}, z_{n_r+2}, \ldots, z_{n_r+n_i}\}. \tag{3}$$

To illustrate, consider that the poles of the ARMAX model are $\aleph = \{-0.1, 0.2, 0.2, 0.1+0.2i, 0.1-0.2i\}$, then $p_1 = 0.1, p_2 = 0.2, p_3 = 0.2, p_4 = 0.1+0.2i$ with i the imaginary number. The damping ratios and natural frequencies can then be evaluated as:

$$\zeta_i = \frac{\left|\mathrm{Re}\{\ln(p_i)\}\right|}{|\ln(p_i)|} \qquad \text{and} \qquad \omega_{n,i} = \frac{\left|\ln(p_i)\right|}{h}, \quad \forall p_i \neq 0, 1, \tag{4}$$

with h the sample period. If $p_i = \{0, 1\}$ then $\zeta_i = 1$. However, the parameter vector θ_a does not contain the damping ratios although this is necessary, as will be explained later. Therefore, a new parameterization of the polynomial $a(z,\theta_a)$ will be introduced:

$$a(z,\theta_\zeta) = \prod_{i=1}^{n_i} \left(z^2 - 2e^{-\zeta_i \omega_{n,i} h} \cos(\omega_{n,i}\sqrt{1-\zeta_i^2}h) z + e^{-2\zeta_i \omega_{n,i} h} \right) \prod_{j=1}^{n_r} \left(z - \mathrm{sign}(z_j) e^{-\omega_{n,j} h} \right), \tag{5}$$

with z_j the real valued pole location and $\omega_{n,j}$ its corresponding natural frequency. The natural frequency and damping coefficient that correspond to each complex pole pair are defined as $\omega_{n,i}$ and ζ_i, respectively. Note that $a(z,\theta_a)$ in (1) is equal to $a(z,\theta_\zeta)$ in (5), but only parameterized differently. The number of parameters in each polynomial is equivalent. As shown below, using system identification, the parameter vectors $a(z,\theta_a), b(z,\theta_b), c(z,\theta_c)$ are found, hence a dynamical model that estimates the network can be defined (see (1)). The damping ratios and natural frequencies of this model can be found using (4) and subsequently, the newly parameterized polynomial $a(z,\theta_\zeta)$ in (5) can be evaluated. A new parameter vector is defined as:

$$\rho = \begin{pmatrix} \theta_b^T & \theta_c^T & \theta_\zeta^T \end{pmatrix}^T \in \mathbb{R}^{n_b+n_c+n_\zeta}. \tag{6}$$

In order to perform system identification, the network needs to be excited. This is carried out via the white noise signals $e(t)$ and probing signal $u(t)$. The former cannot be chosen as it represents unknown random load changes, however, the probing signal $u(t)$ can be designed. In the following section, a method for doing so will be summarized.

Probing Signal Design Method

In this work, we adopt a multisine parameterization for the probing signal $u(t)$ and its power spectrum $\Phi_u(\omega)$:

$$u(t) = \sum_{r=1}^{M} A_r \cos(\omega_r t + \varphi_r), \qquad \Phi_u(\omega) = \frac{\pi}{2} \sum_{r=1}^{M} A_r^2 \Big(\delta(\omega-\omega_r) + \delta(\omega+\omega_r) \Big), \tag{7}$$

with $\delta(\bullet)$ the Dirac function and ω the frequency. Furthermore, $A_r, \omega_r, \varphi_r, M$ are the user-defined magnitude, frequency and phase of the r^{th} sinusoidal component, respectively, and M the number of frequency components taken into account in the optimization problem. Note that in [11], the authors find φ_r to improve estimation accuracy. The framework used in this work will determine the amplitudes A_r in an optimal way, while the φ_r will be chosen randomly.

The following optimization problem is solved to determine the amplitudes A_r of the probing signal $u(t)$:

$$\begin{aligned} \min_{A_r^2(r=1,2,\ldots,M)} \quad & \frac{c_1}{2}\sum_{r=1}^{M} A_r^2 + \frac{c_2}{2}\sum_{r=1}^{M} A_r^2 |G(i\omega_r,\rho)|^2, \\ \text{subject to} \quad & \begin{pmatrix} \eta_i & e_i^T \\ e_i & P^{-1} \end{pmatrix} > 0, \quad \text{for} \quad i = 1,2,\ldots,n_i, \\ & A_r^2 \geq 0, \qquad\qquad \text{for} \quad r = 1,2,\ldots,M, \end{aligned} \tag{8}$$

with the weighted (weight c_1) first term in the cost representing probing signal's power and the second weighted (weight c_2) term the power in the measurement. The latter is also important to be taken into account because the network should not be excited at its critical modes, as it could lead to large oscillations. Hence, the objective of the optimization procedure is to find the power spectrum that minimizes the system disturbance induced by the probing signal as well as the power in the probing signal. The constraints $A_r^2 \geq 0$ are to ensure positivity for the probing signal's power (see (7)) and the other constraints are to ensure an user defined upper bound η_i on the variance of the damping ratios, *i.e.*, variance$(\zeta_i) < \eta_i$. Furthermore, i is the index of the critical mode of interest and e_i is a unity vector whose i^{th} element is equal to one. Using the Schur complement, the constraint in (8) is equivalent to $e_i^T P e_i < \eta_i$. If P represents the covariance matrix of the identified parameter vector ρ, the latter expression is indeed equivalent to variance$(\zeta_i) < \eta_i$. The optimization problem (8) is a convex optimization problem since, as shown in [12, 13, 14], the inverse P^{-1} of the covariance matrix of the parameter vector ρ is an affine function of A_r^2, the to-be-determined amplitudes. It is necessary to parameterize the identified $\hat{G}(z), \hat{H}(z)$ in ρ (see (6)) due to the constraints on the variance of ζ_i, *i.e.*, ζ_i should be contained in ρ. The reader is referred to [12] for more background information on the optimization problem defined in (8).

As shown in [13, 14], the expression of the covariance matrix P used in (8) requires an initial estimate of the parameter vector ρ. Hence, firstly, a model will be identified from a first batch of data by selecting a manually chosen probing signal. The found $\hat{G}(z), \hat{H}(z)$ can subsequently be used to solve (8) and the outcome, an optimized probing signal $u(t)$, can then be injected in the network to improve the damping ratios estimation for the following batch. This process can be repeated automatically so that the probing signal will be updated according to the time-varying network.

Simulation Results

The employed software includes routines developed in Matlab (for system identification) and the Modelica tool Dymola in combination with the OpenIPSL library [15] (for power system modeling). The studied networks are:

- A modified version of the IEEE 14-bus test network, where a STATCOM is installed in bus 14.
- A modified version of the Klein-Rogers-Kundur's two-area systems. A high voltage direct current (VSC-HVDC) link is connected between buses 7 and 9.

A choice has to be made for probing and measurement locations in the network. For example, the probing signal can be the modulation of the voltage control loop of a static VAR compensator, which results in a modulated reactive power injection [16]. A measurement can be the phase angle difference between two chosen buses in the network as in the case when considering the use of phasor measurement units [17]. There are methods that allow to intelligently choose these locations [18], although in this work, these are determined empirically.

In order to demonstrate the proposed method's effectiveness, two simulation experiments are performed and discussed in the following.

a) Base Experiment

The first simulation contains one experiment that takes t_2 seconds (see Fig. 1). Here, the probing signal $u_{\text{base}}(t)$ is chosen manually such that identified (and validated) $\hat{G}_{\text{base}}(z), \hat{H}_{\text{base}}(z)$ are obtained and corresponding damping coefficients can be evaluated.

b) Optimal Experiment

The second simulation contains two experiments (batches) and its objective is to obtain an equivalent variance on the damping estimation as obtained during the first (base) experiment, though with less disturbance in the network (less power in the probing and measurement signals). The two experiments in this simulation each take t_1 seconds, with $t_2 = 2t_1$ (see Fig. 1). The following summarizes the optimal experiment:

1. During the first batch, the probing signal $u_{\text{base}}(t)$ for $t = t_0, t_0+1, \ldots, t_1$ is applied (denoted as $u_1(t)$).
2. The collected measurements $y(t)$ until t_1 are then used to identify $\hat{G}_1(z), \hat{H}_1(z)$ so that consequently P_1 can be evaluated.
3. The problem given in (8) is solved with $\eta_i^{-1} = \left(e_i^T P_{\text{base}} e_i\right)^{-1} - \left(e_i^T P_1 e_i\right)^{-1}$ for $i = 1, \ldots, n_i$, resulting in an optimized probing signal $u_{\text{opt}}(t)$.
4. During the second batch, $u_{\text{opt}}(t)$ for $t = t_1+1, \ldots, t_2$ is applied and the collected measurements are used to identify $\hat{G}_2(z), \hat{H}_2(z)$ so that consequently P_2 can be evaluated.

It should be clear that the upper bound η_i in the third step is set to a value, which will ensure that the optimal experiment combining the manually chosen (during first t_1 seconds) and the optimized probing signal (during last t_1 seconds) yields the same variance as the one obtained in the base experiment (P_{base}).

Figure 1 schematically depicts the base and optimal experiments.

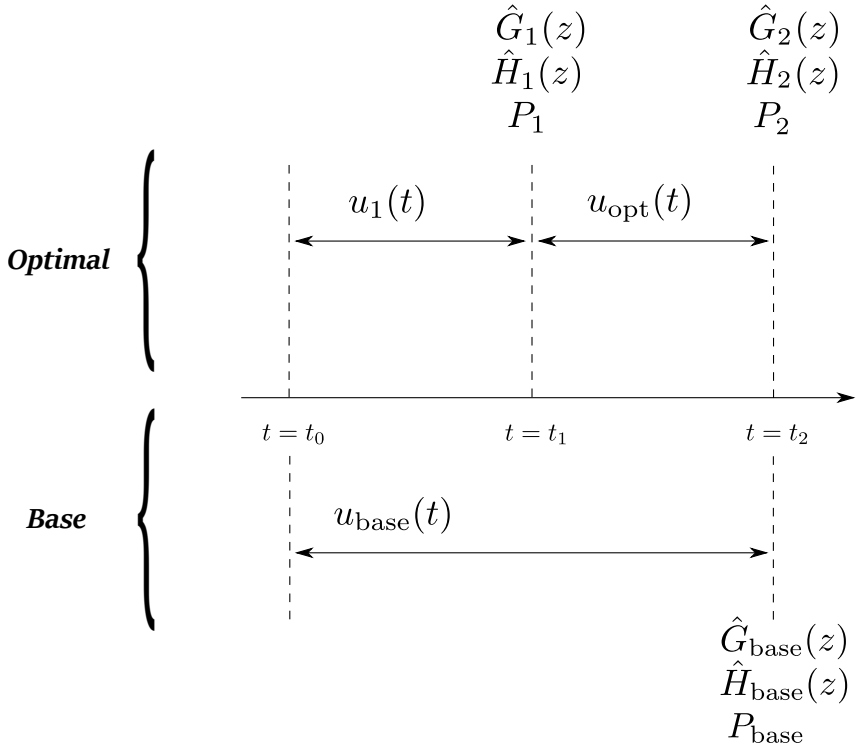

Fig. 1: Schematic representation of the two simulation experiments that are performed in order to show the effectiveness of the proposed probing design method. The objective is to obtain an equivalent variance during both experiment, though with less disturbance in the network during the optimal experiment.

IEEE 14-bus network

Reactive power $u(t)$ will be injected at bus 12, the random load changes $e(t)$ with standard deviation 0.01 in bus 14 and the measurement $y(t)$ is chosen to be the angle difference between bus 1 and bus 8. Hence the objective is to identify a model that estimates the dynamical behavior between reactive power injected at bus 12 and angle difference between the buses 1 and 8. The IEEE 14-bus test network is schematically depicted in Fig. 2.

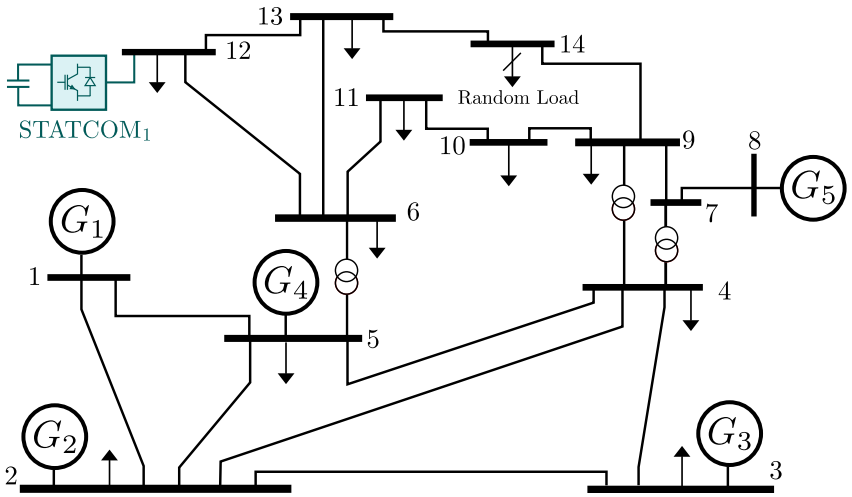

Fig. 2: Schematic representation of the IEEE 14-bus test network.

Table I provides the parameters that are used during the simulations. The parameters $n_\zeta, n_b, n_c, n_k, h$ are empirically found such that an identified and validated $\hat{G}_{\text{base}}(z)$ and $\hat{H}_{\text{base}}(z)$ are found. The parameter N represents the number of used data samples for identifying the model in the base experiment. Hence this parameter is for each batch in the optimal experiment $N/2$.

Table I: Parameters that are used in the IEEE-14 test network.

Parameter	t_0	t_1	t_2	N	h	n_ζ	n_b	n_c	n_k	M	ω_r	c_1	c_2
Value	0	120	240	1200	0.1	8	4	4	0	30	[0.1 3] (Hz)	1	0

The manually found probing signal $u_{\text{base}}(t)$ contains empirically found amplitudes $A_r = 0.02$. A linear spaced $\omega_r \in [0.1\ 3]$ (Hz) with $M = 30$ (see (7)). In general, this frequency range must be chosen such that it contains the dominant modes. This knowledge is generally known for a network from simulation models or spectral analysis on measurements. For this experiment, which takes $t_2 = 240$ seconds, $\hat{G}_{\text{base}}$ and $\hat{H}_{\text{base}}$ (see (1)) are estimated and consequently, the variance P_{base} can be evaluated.

In the first $t_1 = 120$ seconds of the optimal experiment, the same probing signal as used in the first base experiment is applied to the network. The collected measurement until $t_1 = 120$ seconds are then used to identify $\hat{G}_1$ and $\hat{H}_1$. The estimated model is then used to solve (8) with $\omega_r \in [0.1\ 3]$ (Hz) with $M = 30$. The upper bounds η_i are set to a value, which will ensure that the experiment combining the manually chosen signal (during first 120 seconds) and the optimal signal (during last 120 seconds) yields the same variance as the one obtained in the first experiment (manually chosen probing signal during 240 seconds). From $t_1 = 120$ to $t_2 = 240$, the found optimal probing signal is applied and measurements are collected. At $t_2 = 240$, the pair $(\hat{G}_2, \hat{H}_2)$ is identified from which the damping is again evaluated.

The second (optimal) experiment results are depicted in Fig. 3. Here, the first subplot depicts the measurement $y(t)$ (blue) and the simulation output from the estimated ARMAX model $(\hat{y}(t))$ (red). The

depicted "fit" value is a measure of how well $(\hat{y}(t))$ matches with $(y(t))$ and it is evaluated as:

$$\text{fit} = \left(1 - \frac{\sqrt{\sum_{t=1}^{N} |y(t) - \hat{y}(t)|^2}}{\sqrt{\sum_{t=1}^{N} |y(t) - \bar{y}|^2}}\right), \tag{9}$$

with $\bar{y}$ the mean over time of the measurement $y(t)$.

The second subplot shows the probing signal $u(t)$. Note that there is a difference in probing between $t_0 = 0$ until $t_1 = 120$ (manual probing) and $t_1 = 120$ until $t_2 = 240$ (optimal probing). In the third and fourth subplot, the minimum estimated damping ($\hat{\zeta}_{\text{min}}$) and its corresponding natural frequency ($\hat{\omega}_{\text{min}}$)

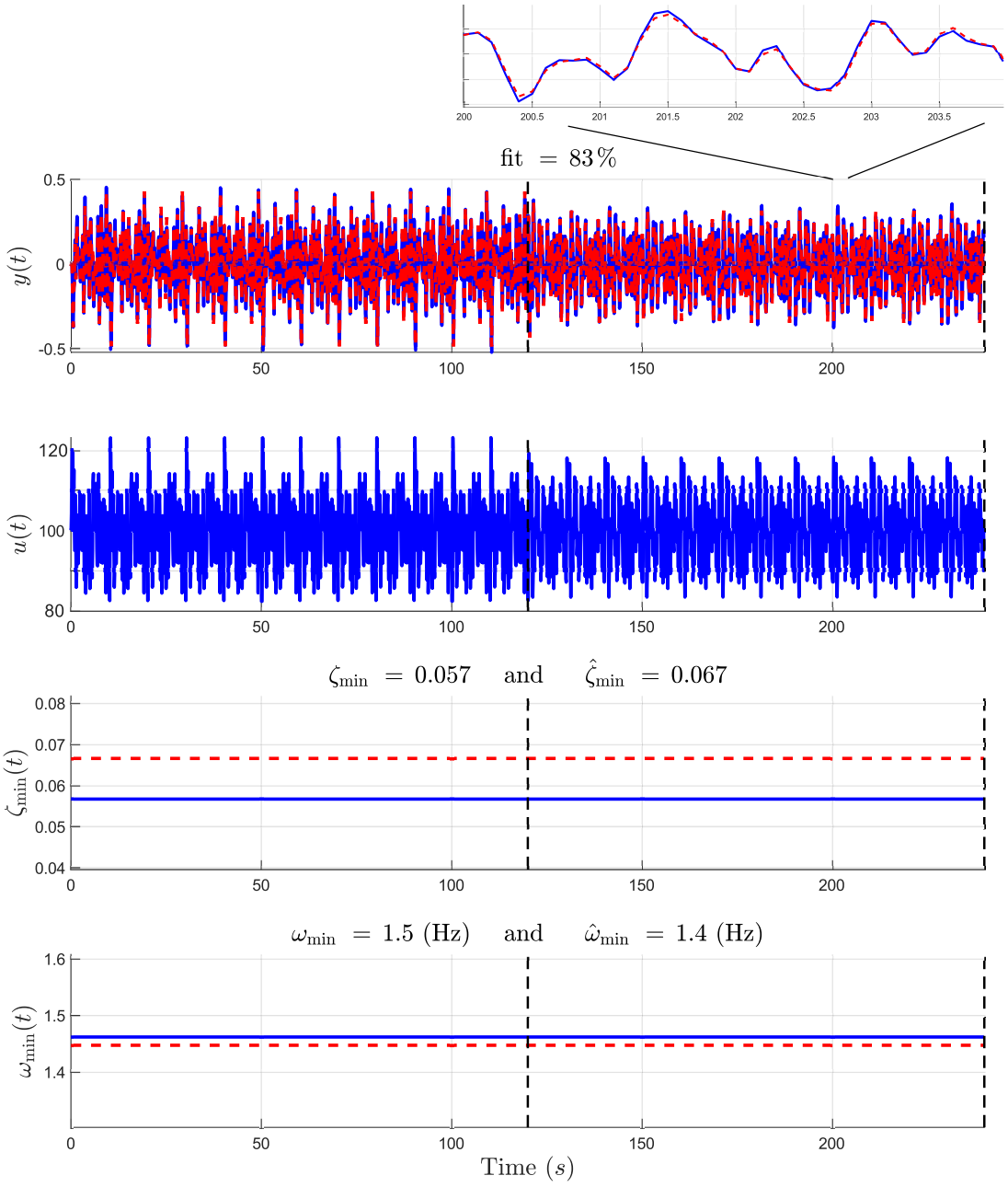

Fig. 3: Identification results obtained with manually chosen (first 120 seconds) and optimal (last 120 seconds) probing signal. The estimated values are indicated in red, while the "true" values obtained from linearizing the simulated model in Dymola (considered as the reality in this work) are indicated in blue. The units of $u(t)$ are in MW.

are depicted, respectively. These estimations are given in red dashed, while the minimum damping and its corresponding frequency obtained from linearizing the simulation model in Dymola, are depicted in blue ($\zeta_{\min}, \omega_{\min}$). These are regarded as the network's true values.

The probing signal's and measurement average power are in the optimal experiment approximately 5% and 20% lower, respectively, compared to the base experiment. Additionally, the manually chosen and optimal probing signals are both applied for 50 batches in order to verify if the estimation's accuracy is ensured (model validation). Over these 50 batches, both types of experiments yield estimates with a sample variance that is very close to the desired one (the differences are among other factors due to the non-linearity of the simulated model).

Kundur network with HVDC link

The probing signal $u(t)$ is the active power that is injected via the VSC-HVDC link in the network. The angle difference between bus 7 and 9 is defined as the measurement $y(t)$ and the random load change $e(t)$ with standard deviation $5 \cdot 10^{-4}$ is applied in bus 2. The objective is to identify a model $\hat{G}(z)$ between the active power of the HVDC link and the angle difference between bus 7 and 9, and a noise model $\hat{H}(z)$ from which the damping coefficients can be evaluated.

The parameters that are used in the Kundur case are given in Table II. Recall that the parameter N is the number of used data samples for identifying the model in the base experiment. Hence this parameter is for each batch in the optimal experiment $N/2$.

Table II: Parameters that are used in the Kundur case study with HVDC link.

Parameter	t_0	t_1	t_2	N	h	n_ζ	n_b	n_c	n_k	M	ω_r	c_1	c_2
Value	0	60	120	2400	0.05	4	4	2	1	30	[0.1 3] (Hz)	1	0

The manually found probing signal $u_{\text{base}}(t)$ contains empirically found amplitudes $A_r = 0.03$. A linear spaced $\omega_r \in [0.1\ 3]$ (Hz) with $M = 30$ (see (7)). For this experiment, which takes $t_2 = 120$ seconds, $\hat{G}_{\text{base}}$ and $\hat{H}_{\text{base}}$ (see (1)) are estimated and consequently, the variance P_{base} can be evaluated.

As in the previous case, a manually chosen multisine is applied in the first t_1 seconds of the optimal experiment. Using this data up to t_1 seconds, a model pair $(\hat{G}_1, \hat{H}_1)$ is identified, which is used to solve the problem given in (8). The outcome is a new set of amplitudes for the multisine that is applied in the second part of the optimal experiment. The empirically found multisine amplitudes and the optimal ones can be found in Fig 4.

The optimal experiment time-domain results are depicted in Fig. 5. Here, just as in the previous case, the first subplot depicts the measurement $y(t)$ (blue) and the simulation output from the identified ARMAX model (red). The second subplot shows the optimal probing signal $u(t)$, which is the active power injected through the HVDC link. In the third and fourth subplot, the minimum estimated damping ($\hat{\zeta}_{\min}$) and its corresponding natural frequency ($\hat{\omega}_{\min}$) are depicted, respectively. These estimations are given in red dashed, while the minimum damping and its corresponding frequency obtained from linearizing the simulation model in Dymola, are depicted in blue ($\zeta_{\min}, \omega_{\min}$). These are regarded as the network's true values.

The probing signal's and measurement average power are in the optimal experiment approximately 90% and 15% lower, respectively, compared to the base experiment. In this test case, the identified models are validated by ensuring that the 1-standard deviation value of the estimated parameters is below the 5% of its nominal value. This value is given by the `present.m` function in Matlab.

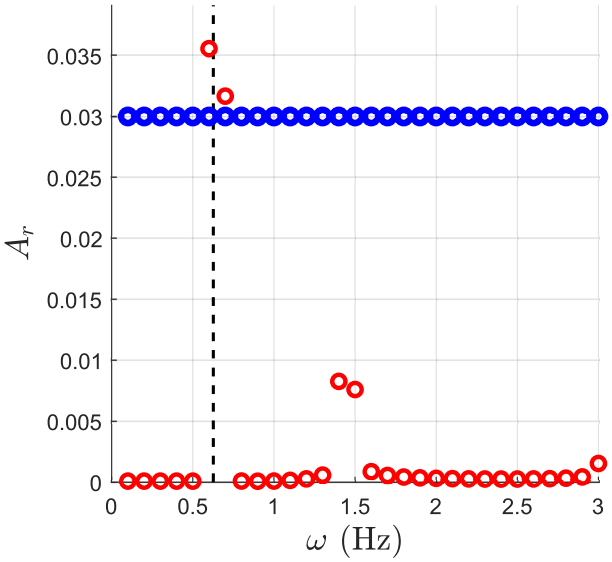

Fig. 4: The amplitudes A_r of the multisine signal (7) that is used in the first part of the optimal experiment (blue), and that is used in the second part of the optimal experiment (red). Note that the amplitudes plotted in red are found by solving the optimization problem given in (8). The vertical dashed line indicates the frequency of the true inter-area mode.

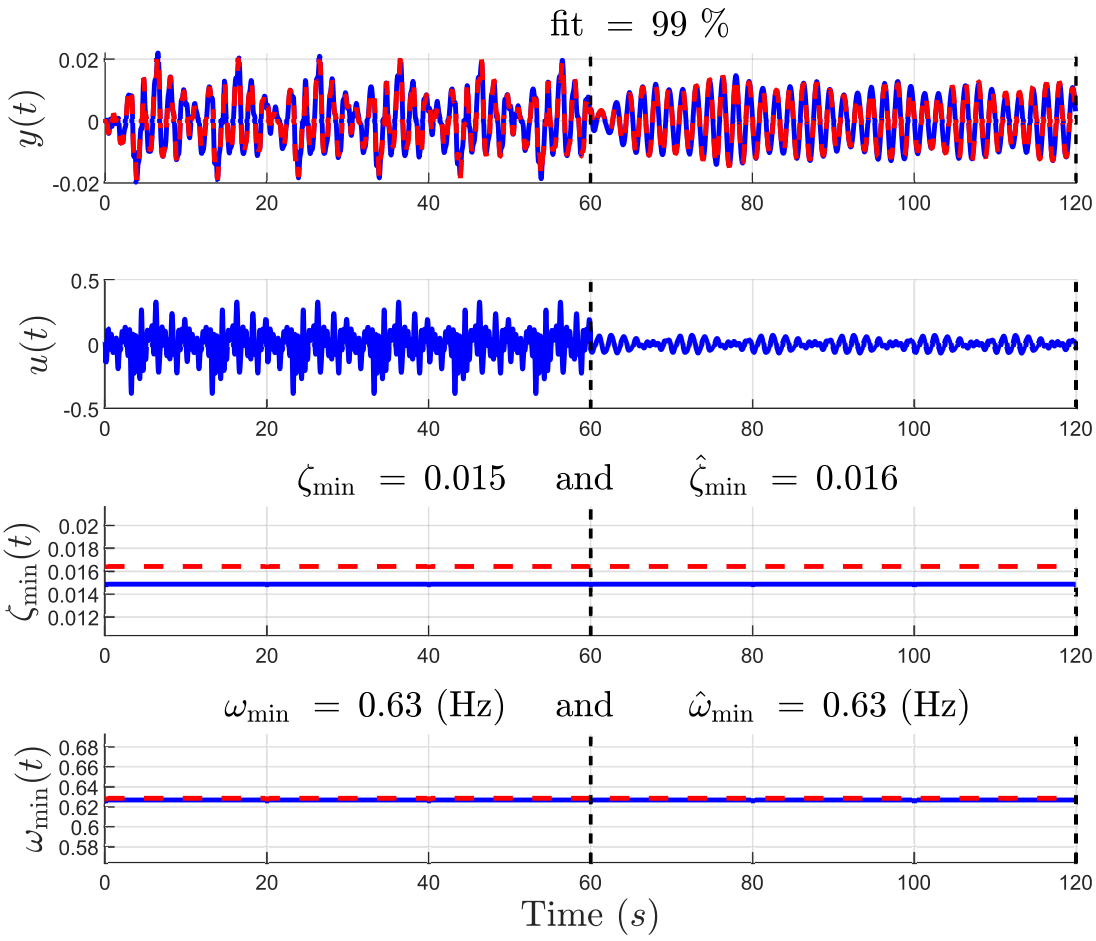

Fig. 5: Identification results obtained with manually chosen (first 60 seconds) and optimal (last 60 seconds) probing signal. The estimated values are indicated in red. The "true" values, that are obtained from linearizing the simulated model in Dymola (considered as the reality in this work), are indicated in blue. The signal $u(t)$ has MW as units and its value is plotted around an equilibrium value.

Conclusions

Oscillations that may lead to instabilities in a power network can potentially be circumvented when having an accurate damping coefficient estimation that helps in guiding corrective actions or to employ closed-loop damping control. The idea is that, when the estimated damping is below a certain threshold, damping control has to be activated in order to increase the damping value. This work presented a method that provides damping estimations with guaranteed accuracy, while minimizing the perturbations in the network. The method combines system identification and optimal probing signal design. An identified model is used to evaluate an optimal probing signal, which is then applied. This paper shows that, for two simulated networks in Dymola, the estimation's accuracy can be ensured. At the same time, the perturbation introduced in the network can be significantly reduced compared to the case where no probing design method has been used. In future work, power hardware in the loop experiments are planned to further test the proposed framework. In addition, the optimal probing design optimization can be explored more by investigating the effect of the tuning variables c_1, c_2. Also, it is planned to test the framework on larger networks such as the Nordic 44 model.

References

[1] F. Galvan and P. Overholt, "The intelligent grid enters a new dimension," *T&D World*, 2014.

[2] D. N. Kosterev, C. W. Taylor, and W. A. Mittelstadt, "Model validation for the August 10," *Trans. Power Syst, vol. 14(3), pp. 967-979*, 1999.

[3] P. Kundur, M. Klein, G. J. Rogers, and M. S. Zywno, "Application of power system stabilizers for enhancement of overall system stability," *Trans. Power Syst, vol. 4(2), pp. 614-626*, 1989.

[4] J. F. Hauer and J. R. Cresap, "Measurement and modeling of pacific AC intertie response to random load switching," *Transactions on Power Apparatus and Systems, vol. 100(1), pp. 353-359*, 1981.

[5] N. Zhou, J. F. Hauer, and J. W. Pierre, "Initial results in power system identification from injected probing signals using a subspace method," *Trans. Power Syst, vol. 21(3), pp. 1296-1302*, 2006.

[6] S. A. N. Sarmadi and V. Venkatasubramanian, "Inter-area resonance in power systems from forced oscillations," *Trans. Power Syst, vol. 31(1), pp. 378-386*, 2016.

[7] X. Du, A. Engelmann, Y. Jiang, T. Faulwasser, and B. Houska, "Optimal experiment design for AC power systems admittance estimation," *arXiv*, 2019.

[8] M. Donnelly, D. Trudnowski, J. Colwell, J. Pierre, and L. Dosiek, "RMS-energy filter design for real-time oscillation detection," *Power & Energy Society General Meeting*, 2015.

[9] D. Kosterev, J. Burns, N. Leitschuh, J. Anasis, A. Donahoo, D. Trudnowski, M. Donnelly, and J. Pierre, "Implementation and operation experience with oscillation detection application at Bonneville power administration," *Grid of the Future Symposium*, 2016.

[10] J. F. Hauer and F. Vakili, "An oscillation detector used in the BPA power system disturbance monitor," *Trans. Power Syst, vol. 5(1), pp. 74-79*, 1990.

[11] J. W. Pierre, N. Zhou, F. K. Tuffner, J. F. Hauer, and D. J. Trudnowski, "Probing signal design for power system identification," *Trans. Power Syst, vol. 25(2), pp. 835-843*, 2010.

[12] V. Peric, X. Bombois, and L. Vanfretti, "Optimal multisine probing signal design for power system electromechanical mode estimation," *Hawaii International Conference on System Sciences*, 2017.

[13] X. Bombois, G. Scorletti, M. Gevers, P. M. J. van den Hof, and R. Hildebrand, "Least costly identification experiment for control," *Automatica, vol. 42(10), pp. 1651-1662*, 2006.

[14] L. Ljung, *System identification: theory for the user*. Prentice Hall, 1999.

[15] M. Baudette, M. Castro, T. Rabuzin, J. Lavenius, T. Bogodorova, and L. Vanfretti, "OpenIPSL: Open-Instance Power System Library - Update 1.5 to "iTesla Power Systems Library (iPSL): A Modelica library for phasor time-domain simulations"," *SoftwareX, vol. 7, pp. 2352-7110*, 2018.

[16] J. C. Gonzalez-Torres, J. Mermet-Guyennet, S. Silvant, and A. Benchaib, "Power system stability enhancement via VSC-HVDC control using remote signals: application on the Nordic 44-bus test system," *International Conference on AC and DC Power Transmission*, 2019.

[17] L. Vanfretti, J. H. Chow, S. Sarawgi, and B. Fardanesh, "A phasor-data-based state estimator incorporating phase bias correction," *Trans. Power Syst, vol. 26(3), pp. 111-119*, 2011.

[18] V. Peric, X. Bombois, and L. Vanfretti, "Optimal signal selection for power system ambient mode estimation using a prediction error criterion," *Trans. Power Syst, vol. 31(4), pp. 2621-2633*, 2016.